

ENCLOSURE 1-NP
TO LD-82-054
STATISTICAL COMBINATION
OF
UNCERTAINTIES

Combination of System Parameter Uncertainties
In Thermal Margin Analyses for SYSTEM 80

Combustion Engineering, Inc.
Windsor, Connecticut

8205180484

LEGAL NOTICE

THIS REPORT WAS PREPARED AS AN ACCOUNT OF WORK SPONSORED BY COMBUSTION ENGINEERING, INC. NEITHER COMBUSTION ENGINEERING NOR ANY PERSON ACTING ON ITS BEHALF:

A. MAKES ANY WARRANTY OR REPRESENTATION, EXPRESS OR IMPLIED INCLUDING THE WARRANTIES OF FITNESS FOR A PARTICULAR PURPOSE OR MERCHANTABILITY, WITH RESPECT TO THE ACCURACY, COMPLETENESS, OR USEFULNESS OF THE INFORMATION CONTAINED IN THIS REPORT, OR THAT THE USE OF ANY INFORMATION, APPARATUS, METHOD, OR PROCESS DISCLOSED IN THIS REPORT MAY NOT INFRINGE PRIVATELY OWNED RIGHTS; OR

B. ASSUMES ANY LIABILITIES WITH RESPECT TO THE USE OF, OR FOR DAMAGES RESULTING FROM THE USE OF, ANY INFORMATION, APPARATUS, METHOD OR PROCESS DISCLOSED IN THIS REPORT.

STATISTICAL COMBINATION OF UNCERTAINTIES

Combination of System Parameter Uncertainties
in Thermal Margin Analysis for System 80

ABSTRACT

This report describes the methods used to statistically combine system parameter uncertainties in the thermal margin analyses for the System 80 cores. A detailed description of the uncertainty probability distributions and response surface techniques used is presented. This report demonstrates that there will be at least 95% probability with at least 95% confidence that the limiting fuel pin will avoid departure from nucleate boiling (DNB) so long as the minimum DNB ratio found with the best estimate design CETOP-D model remains at or above 1.22.

TABLE OF CONTENTS

<u>Title</u>	<u>Page</u>
Abstract	i
Table of Contents	ii
List of Figures	iv
List of Tables	v
Nomenclature and Abbreviations	vi
Subscripts and Superscripts	vii
1.0 Summary of Results	1-1
2.0 Introduction	2-1
2.1 Deterministic Method	2-2
2.2 Statistical Method	2-2
3.0 Sources of Uncertainty	3-1
3.1 State Parameters Used in the Study	3-1
3.1.1 Method for Selecting State Parameters	3-2
3.1.2 Axial Shape Sensitivity	3-3
3.1.3 Pressure and Temperature Sensitivity	3-3
3.1.4 Primary System Flowrate Sensitivity	3-3
3.1.5 Most Adverse State Parameters	3-4
3.2 Radial Power Distribution	3-4
3.3 Inlet Flow Distribution	3-4
3.4 Exit Pressure Distribution	3-4
3.5 Enthalpy Rise Factor	3-5
3.6 Heat Flux Factor	3-5
3.7 Clad O.D.	3-5
3.8 Systematic Pitch Reduction	3-6
3.9 Fuel Rod Bow	3-6

TABLE OF CONTENTS (con't)

<u>Title</u>	<u>Page</u>
3.10 CHF Correlation	3-6
3.11 TORC Code Uncertainty	3-7
4.0 MDNBR Response Surface	4-1
4.1 TORC Model Used	4-1
4.2 Variables Used	4-1
4.3 Experiment Design	4-2
4.4 Design Matrix	4-3
4.5 Response Surface	4-3
5.0 Combination of Probability Distribution Functions	5-1
5.1 Method	5-1
5.2 Results	5-2
5.3 Analytical Comparison	5-2
6.0 Application to Design Analysis	6-1
6.1 Statistically Derived MDNBR Limit	6-1
6.2 Adjustments to Statistically Derived MDNBR Limit	6-1
6.3 Application to TORC Design Model	6-2
7.0 Conclusions	7-1
7.1 Conservatisms in the Methodology	7-1
8.0 References	8-1
Appendix	
Appendix A: Detailed TORC Analyses Used to Generate Response Surface	A-1

LIST OF FIGURES

<u>Fig. No.</u>	<u>Title</u>	<u>Page</u>
3-1	Inlet Flow Distribution Used to Generate Response Surface	3-8
3-2	Exit Pressure Distribution Used to Generate Response Surface	3-9
3-3	Core Wide Radial Power Distribution Used to Generate Response Surface	3-10
3-4	Hot Assembly Radial Power Distribution Used to Generate Response Surface	3-11
3-5	Channel Numbering Scheme for Stage 1 TORC Analysis to Generate Response Surface	3-12
3-6	Intermediate (2nd Stage) TORC Model Used In Generating Response Surface	3-13
3-7	Subchannel (3rd Stage) TORC Model Used in Generating Response Surface	3-14
5-1	Resultant MDNBR Probability Distribution Function	5-4

LIST OF TABLES

<u>Table No.</u>	<u>Title</u>	<u>Page</u>
3-1	Ranges of Operating Conditions for Which Response Surface is Valid	3-15
3-2	Determination of the Most Sensitive Axial Shape Index	3-16
3-3	Determination of the Most Sensitive Primary System Inlet Pressure and Temperature	3-18
3-4	As-Built Gap Width Data	3-20
3-5	Inlet Mass Velocity Ratio	3-21
4-1	System Parameters Included as Variables in the Response Surface	4-4
4-2	Coefficients for MDNBR Response Surface	4-5
5-1	Probability Distribution Functions Combined by SIGMA	5-5
A-1	Coded Set of Detailed TORC Cases Used to Generate Response Surface	A-2
A-2	Comparison of TORC and Response Surface MDNBR for Cases Used to Generate Response Surface	A-3

NOMENCLATURE AND ABBREVIATIONS

b	coefficient in response surface
c	constant in response surface
f	arbitrary functional relationship
k	number of independent variables in response surface
n	number of items in a sample
p.d.f.	probability distribution function
psd	pounds per square foot
psia	pounds per square inch (absolute)
x	system parameter
y	state parameter
z	MDNBR values predicted by response surface
ASI	axial shape index (defined in Table 3-2)
CE	Combustion Engineering
CHF	Critical Heat Flux
DNB	Departure from Nucleate Boiling
DNBR	Departure from Nucleate Boiling Ratio
F	Fahrenheit
F_q	engineering heat flux factor
MDNBR	Minimum Departure from Nucleate Boiling Ratio
T	temperature
T-H	thermal-hydraulic
α	constant used to code system parameters (Table 4-1)
β	constant used to code system parameters (Table 4-1)
η	coded value of system parameters (Table 4-1)
μ	mean
σ	standard deviation
Δ	denotes difference between two parameters

subscripts

$\vec{}$ denotes vector quantity

i index

in conditions at reactor core inlet

j index

superscripts

\wedge denotes estimate

$^\circ$ degrees

$-$ average value

1.0 Summary of Results

Methods were developed to combine statistically the uncertainties in reference thermal margin (detailed TORC) analyses. These methods were applied to the System 80 core. This work demonstrated that there will be at least 95% probability with at least 95% confidence that the limiting fuel pin will avoid departure from nucleate boiling (DNB) so long as the Minimum DNBR Ratio (MDNBR) found with the best-estimate design CETOP-D model remains at or above 1.22. The 1.22 MDNBR limit includes allowances for reference analysis input uncertainties but does not take into account uncertainties in operating conditions (e.g., monitoring uncertainties).

2.0 Introduction

C-E's thermal margin methodology for System 80 has been modified by the application of statistical methods. This report focuses on the statistical combination of reference thermal-hydraulic (T-H) code input uncertainties. This combination was accomplished by the generation of a Minimum DNBR (MDNBR) response surface and the application of Monte Carlo methods.

A complete description of the methods used in the statistical combination is provided in this report. The remainder of this section outlines the previous deterministic and the new statistical thermal margin methods. Section 3.0 describes the sources of uncertainty that were considered in this effort. Section 4.0 describes the MDNBR response surface. The application of Monte Carlo Methods is discussed in Section 5.0, and results are presented. Finally, Section 6.0 describes the changes in design analyses that result from this work, in particular, the resultant MDNBR limit of 1.22 which accommodates the T-H uncertainties described in this report.

2.1 Deterministic Method

Two types of problem dependent data are required before a detailed T-H code can be applied. The first type of data, system parameters, describe the physical system, such as the reactor geometry, pin-by-pin radial power distributions, inlet and exit flow boundary condition, etc. These are not monitored in detail during reactor operation. The second type of data, state parameters, describe the operational state of the reactor. State parameters are monitored while the reactor is in operation and include the core average inlet temperature, primary loop flow rate, primary loop pressure, etc.

C-E thermal margin methods (2-1) utilize the TORC (2-2) and CETOP-D (2-3) codes and the CE-1 CHF correlation (2-4) with two types of models. The first model, detailed TORC, is tailored to yield best estimate MDNBR predictions in a particular fuel assembly for a specific power distribution. Both system and state parameter input are used in a detailed TORC model. The second model, the CETOP-D design model, requires only state parameter data and may be applied to any fuel assembly for any power distribution that is expected to occur during a particular fuel cycle. System parameters are fixed in the design model so that the model will yield either accurate or conservative MDNBR predictions for all operating conditions within a specified range.

Design model MDNBR results are verified by comparison with results from the detailed model of the limiting assembly in the deterministic method. After the design model is shown to yield acceptable (i.e., accurate or conservative) results, additional adjustment factors are applied to account for uncertainties in system parameter input to the detailed model. For example, engineering factors are applied to the hot subchannel of the design model to account for fuel fabrication uncertainties. These adjustment factors, though arrived at statistically, are applied in a deterministic manner. That is, although each adjustment factor represents a 95/95 probability/confidence limit that the particular parameter deviation from nominal is no worse than described by that factor, all factors are applied simultaneously to the limiting subchannel. This is equivalent to assuming that all adverse deviations occur simultaneously in the limiting subchannel.

2.2 Statistical Method

The probability of all adverse system parameter deviations from nominal occurring simultaneously in the limiting subchannel is extremely remote. With a more reasonable, demonstrably conservative method, the probability of system parameter input being more adverse than specified can be taken into account statistically, as described herein.

The improved methodology involves a statistical combination of system parameter uncertainties with the CHF correlation uncertainties to determine a revised design MDNBR limit. Since uncertainties in system parameters are taken into account in the derivation of the new MDNBR limit, no other allowance need be made for them. A best estimate design CETOP-D model is therefore used with the revised MDNBR limit for thermal margin analysis. This best estimate design model yields conservative or

accurate MDNBR results when compared with a best estimate detailed model. The resultant best estimate design model and increased MDNBR limit ensure with at least 95% probability and at least a 95% confidence level that the limiting fuel pin will avoid departure from nucleate boiling if the predicted MDNBR is not below the limit MDNBR.

3.0 Sources of Uncertainty

Four types of uncertainty are identified in MDNBR predictions from the TORC code:

- i) numerical solution parameter uncertainty
- ii) code uncertainty
- iii) state parameter uncertainty
- iv) system parameter uncertainty

Numerical solution parameters are required input that would not be necessary if analytic methods could be used (e.g., radial mesh size, axial mesh size, convergence criteria, etc.). The uncertainties associated with these parameters are dealt with in a conservative manner (3-1) in C-E's present methodology.

The numerical algorithms in the TORC code represent approximations to the conservation equations of mass, momentum, and energy. Because of the approximations involved, an inherent code uncertainty exists. This uncertainty is implicitly dealt with in the CE-1 CHF correlation as discussed in Section 3.11.

State parameters define the operational state of the reactor. Uncertainties in these parameters are included when the CETOP-D model is incorporated into the operating algorithms.

As explained in Section 2.1, system parameters describe the physical environment that the working fluid encounters. This report establishes the equivalent MDNBR uncertainty that results from a statistical combination of uncertainties in system parameters.

3.1 State Parameters Used in the Study

Generation of a response surface which simultaneously relates MDNBR to both system and state parameters would require an excessive number of detailed TORC analyses. Consequently, a conservative approximation is made and a response surface relating MDNBR to system parameters only is created. To achieve conservatism, it is necessary to generate the surface for that set of state parameters which maximizes the sensitivity of MDNBR to system parameter variations. That is, the response surface can be described as:

$$\text{MDNBR} = g(\underline{x}, \underline{y}_0)$$

where \underline{x} is the vector of system parameters, and

\underline{y}_0 the vector of state parameters, is selected such that

$$\left\| \frac{\partial(\text{MDNBR})}{\partial \underline{x}} \right\| \xrightarrow{\text{maximum}} \underline{y}_0$$

The set of state parameters, y_0 , that satisfies the above relation, is referred to as the most adverse set of state parameters. The generation of the response surface is discussed in Section 4.3.

3.1.1 Method for Selecting State Parameters

Allowable operating parameter ranges are presented in Table 3-1. These ranges are based upon reactor setpoints including measurement uncertainty. The response surface must be valid over these ranges. As indicated above, a single set of operating conditions is chosen from these ranges to maximize the sensitivity of MDNBR to system parameters.

This set of state conditions is determined from detailed TORC analyses in the following manner. Three TORC analyses are performed for a single set of operating conditions. In the first analysis, nominal system parameters are used and the core average heat flux is chosen to yield a MDNBR in the neighborhood of 1.19. A second TORC analysis uses the same heat flux and operating conditions but has all system parameters (i.e., pitch, clad O.D., enthalpy rise) perturbed in an adverse direction (i.e., MDNBR decreases). A third TORC analysis uses the same heat flux and operating conditions but has all system parameters perturbed in an advantageous direction (i.e., MDNBR increases). The MDNBR from the "adversely perturbed" analysis is then subtracted from the "nominal" MDNBR to yield a $\Delta \text{MDNBR}_{\text{ADVERSE}}$ for the chosen set of operating conditions and the same is done for the TORC analysis where system parameters are "perturbed advantageously". That is,

$$\Delta \text{MDNBR}_{\text{ADVERSE}} = \left| \text{"Nominal" MDNBR} - \text{"Adversely Perturbed" MDNBR} \right| \quad (3.1)$$

$$\Delta \text{MDNBR}_{\text{ADVANTAGEOUS}} = \left| \text{"Nominal" MDNBR} - \text{"Advantageous Perturbed" MDNBR} \right| \quad (3.2)$$

The percent change in MDNBR is then determined according to the following relationships:

$$\% \text{ Change}_{\text{ADVERSE}} = \left| \left(\Delta \text{MDNBR}_{\text{ADVERSE}} / \text{"Nominal" MDNBR} \right) \times 100 \right| \quad (3.3)$$

$$\% \text{ Change}_{\text{ADVANTAGEOUS}} = \left| \left(\Delta \text{MDNBR}_{\text{ADVANTAGEOUS}} / \text{"Nominal" MDNBR} \right) \times 100 \right|$$

This process is repeated for several sets of operating conditions to establish the sensitivity of the MDNBR throughout the allowable operating range. Sets of operating conditions used in this sensitivity study are chosen to envelop the required ranges shown in Table 3-1.

The set of state parameter values which maximizes the quantity $(\% \text{ Change}_{\text{ADVERSE}} + \% \text{ Change}_{\text{ADVANTAGEOUS}})$ is chosen as the most sensitive set of state parameter values. This set is referred to as the set of "most adverse" state parameter values and is used in determining the response surface.

Since MDNBR is a smoothly varying function of these state parameters (3-2), it is likely that the theoretical set of most adverse state parameters will be similar to the most adverse set found by the method described above. Similarly, it is also highly unlikely that MDNBR

sensitivities observed with the theoretical most adverse set will differ appreciably from MDNBR sensitivities which occur using the most adverse set found by the above method.

Inlet flow and exit pressure boundary conditions for the model are shown in Fig. 3-1 and 3-2. Core-wide and hot assembly power distributions are shown in Fig. 3-3 and 3-4 respectively. The detailed TORC analysis (3-1) consists of three stages. A core-wide analysis is done on the first stage, in which each fuel assembly near the limiting assembly is modeled as an individual channel. Crossflow boundary conditions from the first stage are applied in the second stage to a more detailed model of the neighborhood around the limiting assembly. Each quadrant of the limiting assembly is represented by a channel in the second stage analysis. Crossflow boundary conditions from the second stage are applied to the subchannel model of the limiting assembly hot quadrant in the third stage, and the MDNBR is calculated. TORC models for the first, second, and third stages of the model used in the sensitivity study are shown in Figures 3-5, 3-6, and 3-7 respectively.

3.1.2 Axial Shape Sensitivity

Detailed TORC analyses as described in Section 3.1.1 are performed to determine the most sensitive ASI to be used in the analysis. Data from these calculations are listed in Table 3-2. The most sensitive ASI is found to be the [] ASI.

3.1.3 Pressure and Temperature Sensitivity

Using the ASI determined in Section 3.1.2, detailed TORC analyses are performed using the method described in Section 3.1.1 to determine the pressure and temperature to be used in defining the Response Surface. Data from this analysis are found in Table 3-3. From these analyses it was determined that the most sensitive pressure and temperature are [] respectively.

3.1.4 Primary System Flowrate Sensitivity

Detailed TORC analyses as described in Section 3.1.1 are performed to determine the most sensitive flowrate to be used in this analysis. Data from these calculations are listed on Table 3-3. The most sensitive flowrate was found to be [] of design flow. (Design flow is equal to 445,600 gpm.)

3.1.5 Most Adverse Parameters

As explained in Section 3.1, the set of state parameters chosen for use in generating the response surface should maximize MDNBR sensitivity to variations in system parameters; this is the most adverse set of state parameters. The most sensitive set of parameters is chosen so that the resultant MDNBR uncertainty will be maximized. This introduces conservatism into the overall treatment.

From Sections 3.1.2, 3.1.3 and 3.1.4, it is seen that the state parameters which maximize MDNBR sensitivity are:



where 100% design flow is 445,600 gpm.

3.2 Radial Power Distribution

Inherent conservatism in the thermal margin modeling methodology makes it unnecessary to account for uncertainties in the radial power distributions that are used in TORC DNB analyses.

3.3 Inlet Flow Distribution

An inlet flow boundary condition is used in detailed TORC analysis. Ratios of the local to core average mass velocity are input for every flow channel in the core wide analysis. The inlet flow distribution used in the detailed TORC cases to generate the Minimum DNBR response surface is shown in Figure 3-1.

[] flow model tests were run to determine the System 80 inlet flow distribution; hence, [] points are available to use in characterizing the probability distribution function (p.d.f.) associated with each of the mass velocity ratios used in the inlet flow boundary condition. []

[] deterministic allowances were included in the inlet flow distribution used in detailed TORC analyses to benchmark the System 80 CETOP-D model. The general benchmarking methods are discussed in Reference 3-11.

The deterministic method used to account for inlet flow distribution uncertainty consisted of []

[] The [] of the inlet flow mass velocity ratios for the [] based on flow model test data are shown in Table 3-5 along with the [] which are used to benchmark CETOP-D.

Since inlet flow distribution uncertainties are taken into account using deterministic methods, these uncertainties are not included in the statistical analysis described in this report.

3.4 Exit Pressure Distribution

Sensitivity studies indicate that MDNBR is extremely insensitive to variations in the exit pressure distribution (Ref. 3-4). Consequently, the exit pressure distribution need not be included in the MDNBR response surface.

3.5 Enthalpy Rise Factor

The engineering enthalpy rise factor accounts for the effects of manufacturing deviations in fuel fabrication from nominal dimensions and specifications on the enthalpy rise in the subchannel adjacent to the rod with the MDNBR (3-3). Tolerance deviations in fuel pellet density, enrichment, and diameter averaged over the length of the fuel rods are used to compute this factor.

As-built data for 16x16 fuel were used to generate an enthalpy rise factor distribution characterized by a mean of approximately [] and a standard deviation at 95%+ confidence of [].

3.6 Heat Flux Factor

The engineering heat flux factor is used to take into account the effect on local heat flux of deviations from nominal design and specifications that occur in fabrication of the fuel. Random variation in pellet enrichment, initial pellet density, pellet diameter, and clad outside diameter (O.D.) contribute to the effects represented by the engineering heat flux factor. Tolerance limits and fuel specifications ensure that this factor may be characterized conservatively by a normal p.d.f. with a mean of [] and standard deviation at 95% confidence of [].

3.7 Clad O.D.

Variations in clad diameter change subchannel flow area and also change the local heat flux. The impact of both random and systematic variations in fuel clad O.D. on the local heat flux is accounted for by the engineering factor on heat flux, discussed in Section 3.6. The effect of random variations in clad O.D. on subchannel flow area is included in the rod bow penalty, discussed in Section 3.9. The effect of systematic variations in clad O.D. on the subchannel hydraulic parameters is addressed here.

Manufacturing tolerances on the fuel clad allow for the possibility that the clad diameter will be systematically above nominal throughout an entire fuel assembly. That is to say, the mean as-built value of the clad O.D. may differ from the nominal value. The distribution of the mean clad O.D. for fuel assemblies may be characterized by a normal p.d.f. with a mean equal to the mean clad O.D. and a standard deviation given by the relationship (3-5):

$$\sigma_{\mu} = \sigma \sqrt{\frac{(N-n)}{n(N-1)}}$$

where N is the number of specimens in the parent population and n is the sample size.

As-built data for 16x16 fuel indicate that the maximum systematic clad O.D. is [] inches. Since the adverse effect of clad O.D. variations is already taken into account by the engineering heat flux factor, and use of a less than nominal clad O.D. would increase subchannel flow area, benefiting the MDNBR, the maximum value [] is used in this study. The mean at the 95% confidence level is [] inches and the standard deviation of the mean at the 95% confidence level is [] inches. The double accounting for both the adverse effect of a decrease in clad O.D. in the engineering factor on heat flux and the adverse effect of a systematic increase in clad O.D. on subchannel flow area adds conservatism to the analysis.

3.8 Systematic Pitch Reduction

The rod bow penalty, discussed in Section 3.9, takes into account the adverse effect on MDNBR that results from random variations in fuel rod pitch. The rod bow penalty does not take into account the adverse effect of systematic variations in fuel rod pitch. This systematic pitch reduction effect must be discussed separately.

Manufacturing tolerances on fuel assemblies allow for the possibility that the as-built fuel pitch will be less than nominal throughout an entire fuel assembly. Thus the systematic pitch refers to the mean value of the pitch in an assembly. The systematic pitch distribution is assumed to be a normal distribution characterized by the mean value of the pitch and the standard deviation of that mean value.

As-built gap width data for 16x16 fuel are presented in Table 3-4. The minimum systematic gap width is seen to occur in the AKBTO2 assembly [] and is [] inches. This, combined with the maximum clad O.D. from Section 3.7 indicates that the minimum pitch is [] inches. The mean at the 95% confidence level is [] inches, and the deviation of the mean at the 95% confidence level is [] inches.

3.9 Fuel Rod Bow

The fuel rod bow penalty accounts for the adverse impact on MDNBR of random variations in spacing between fuel rods. The methodology for determining the rod bow penalty is the subject of a C-E topical report (3-6). Appendix G of that report (3-7) applies a formula derived by the NRC (3-7) to compute the rod bow penalty for C-E fuel. The penalty at 20,000 MWD/MTU for C-E's 16x16 fuel is 0.8% in DNBR. This penalty is applied directly to the new MDNBR limit derived in Section 6.

3.10 CHF Correlation

The C-E 1 Critical Heat Flux (CHF) correlation (3-9) (3-10) is used in the TORC code (3-1) to determine whether a departure from nucleate boiling (DNB) will occur. This correlation is based on a set of 731 data points. The mean of the ratio of observed to predicted CHF using the CE-1 correlation is 0.99983, while the standard deviation of that ratio is 0.06757. CHF correlation uncertainty may be characterized by a normal distribution with a mean 0.99983 and standard deviation of 0.06757. This yields a 1.13 MDNBR limit to satisfy the criterion of "95% probability at

the 95% confidence level that the limiting fuel pin does not experience DNB". However, because the NRC staff has not yet concluded its review of the CE-1 correlation, a 5% penalty has been applied; this raises the 95/95 MDNBR limit to 1.19. This penalty may be conservatively treated by displacing the above normal distribution by +0.06 producing a displaced normal distribution with a mean of 1.06 ($.99983 + 0.06$) and the same standard deviation as above.

3.11 TORC Code Uncertainty

The TORC computer code (3-1) represents an approximate solution to the conservation equations of mass, momentum, and energy. Simplifying assumptions were made, and experimental correlations were used to arrive at the algorithms contained in the TORC code. Hence, the code has associated with it an inherent calculational uncertainty. Comparisons between TORC predictions and experimental data (3-1) (3-11) have shown that TORC is capable of adequate predictions of coolant conditions.

As explained in Section 5.0 of Reference (3-11), the TORC code was used to determine local coolant conditions from data obtained during the CE-1 CHF experiments. These local coolant conditions were then used to develop the CE-1 CHF correlation. Thus, any calculational uncertainty in the TORC code is implicitly included in the MDNBR limit that is used with the TORC/CE-1 package in thermal margin analyses.

Figure 3-1

INLET FLOW DISTRIBUTION USED TO GENERATE RESPONSE SURFACE

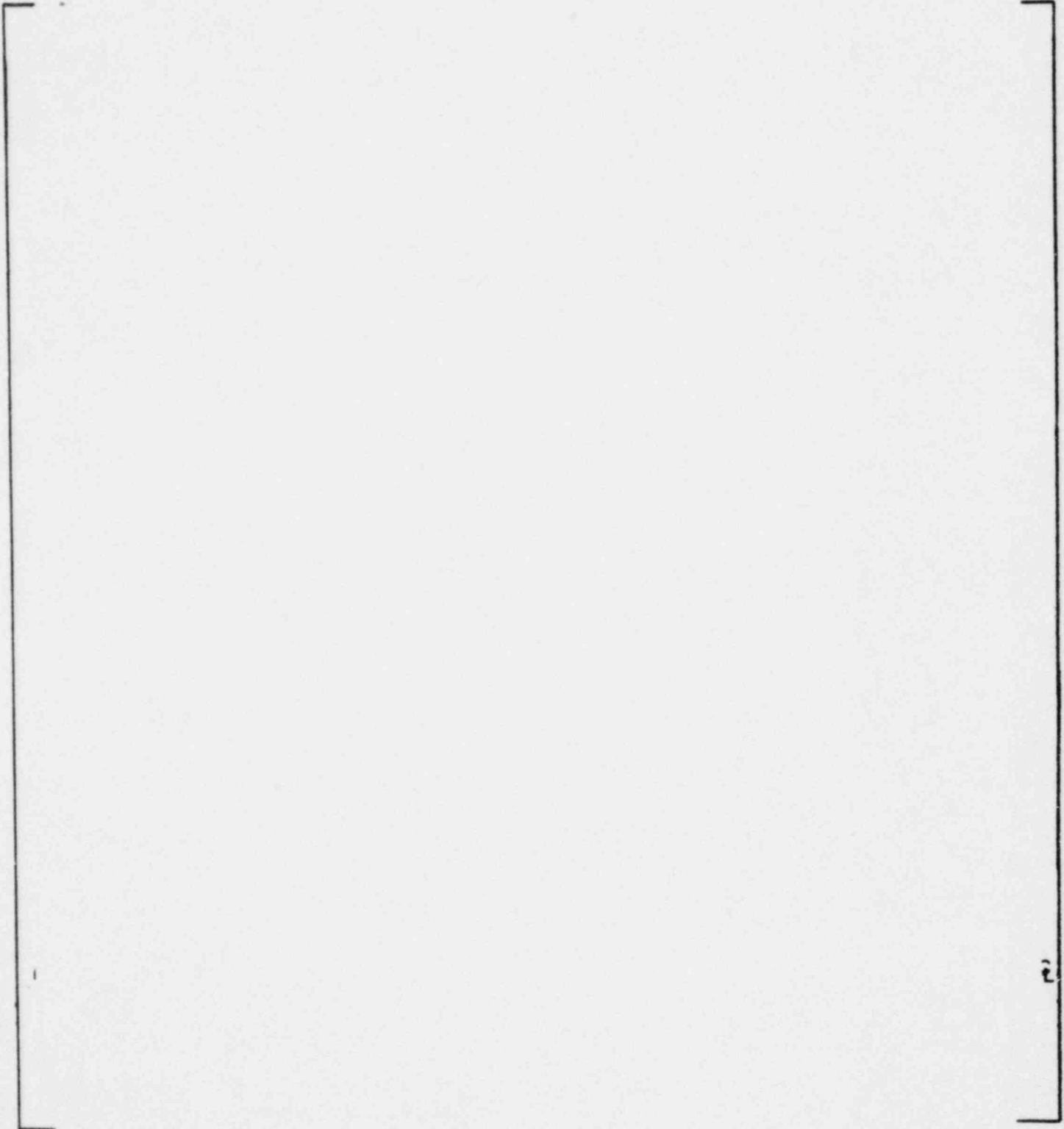


Figure 3-2

CORE EXIT PRESSURE DISTRIBUTION USED TO GENERATE RESPONSE SURFACE

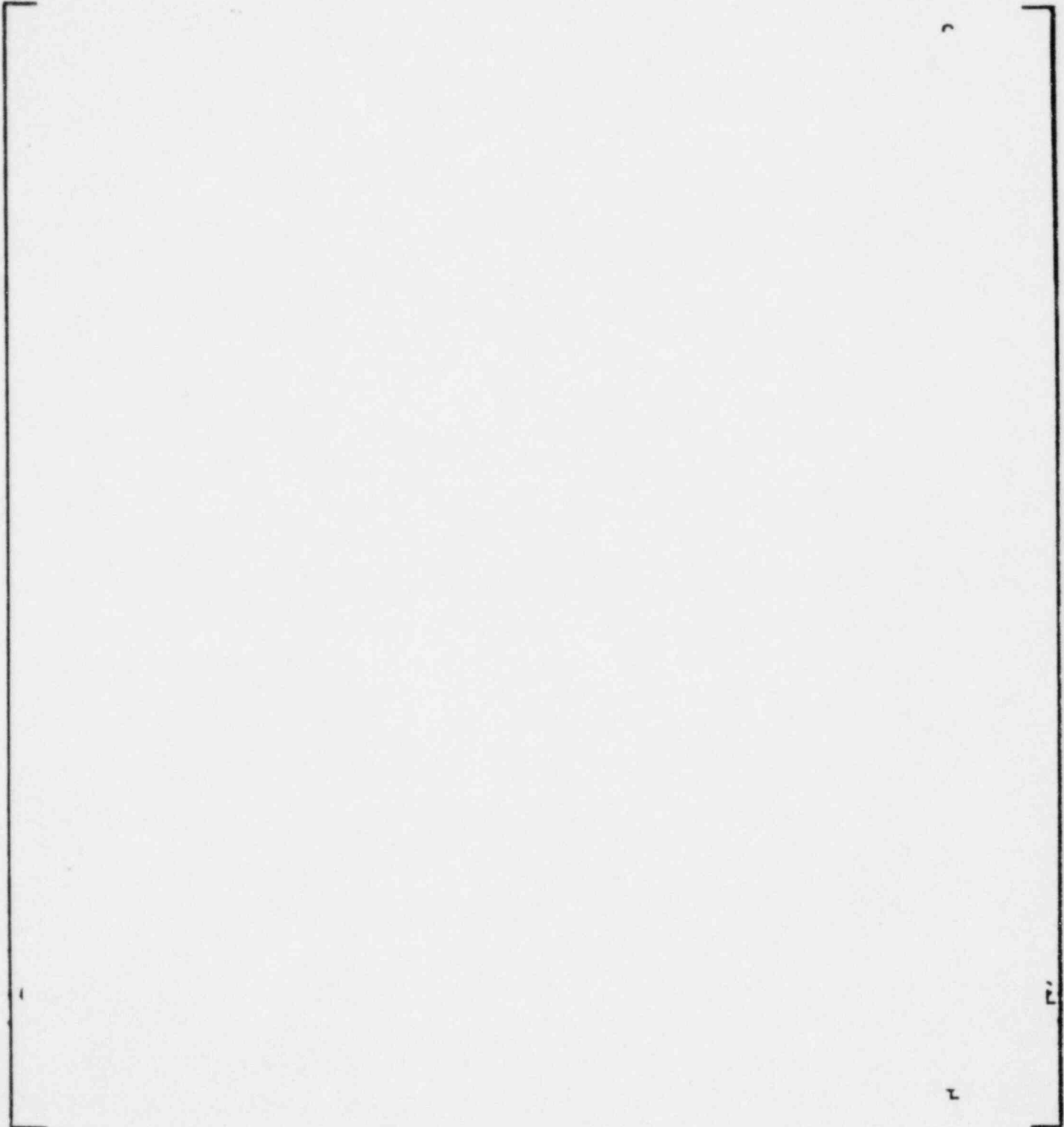


Figure 3-3

CORE WIDE RADIAL POWER DISTRIBUTION USED TO
GENERATE RESPONSE SURFACE

STAGE 1 TORC ANALYSIS
CHANNEL NUMBER

ASSEMBLY AVERAGE
RADIAL PEAKING FACTOR

SEE NOTE
FIGURE 3-5

					1	2	3	4	⊥
					0.6214	0.7988	0.8583	0.8760	
			5	6	7	8	9	10	
			0.6164	0.8874	1.1028	1.0924	1.1875	1.2187	
		11	12	13	14	15	16	17	
		0.7041	1.0931	0.9475	1.1313	0.8671	1.1985	1.2565	
	18	19	20	21	22	23	24	25	
	0.6200	1.0882	1.1759	1.1552	0.9717	1.1152	0.9383	1.0597	
	26	27	28	29	30	31	32	33	
	0.8329	0.9516	1.1610	0.8639	1.1272	0.9625	1.0173	0.6237	
34	35	36	37	38	39	42			
0.6260	1.0990	1.1326	0.9695	1.1332	0.9980	1.1905	0.9509	1.0293	
40			41						
0.7962	1.1004	0.8692	1.1118	0.9669	1.1852	1.2466	1.2038	0.9913	
0.8549	1.1959	1.2073	0.9373	1.0188	0.9473	1.1981	1.0167	1.1645	
0.8719	1.2146	1.2547	1.0675	0.6231	1.0350	0.9947	1.1589	0.8740	⊥
									⊥
									⊥

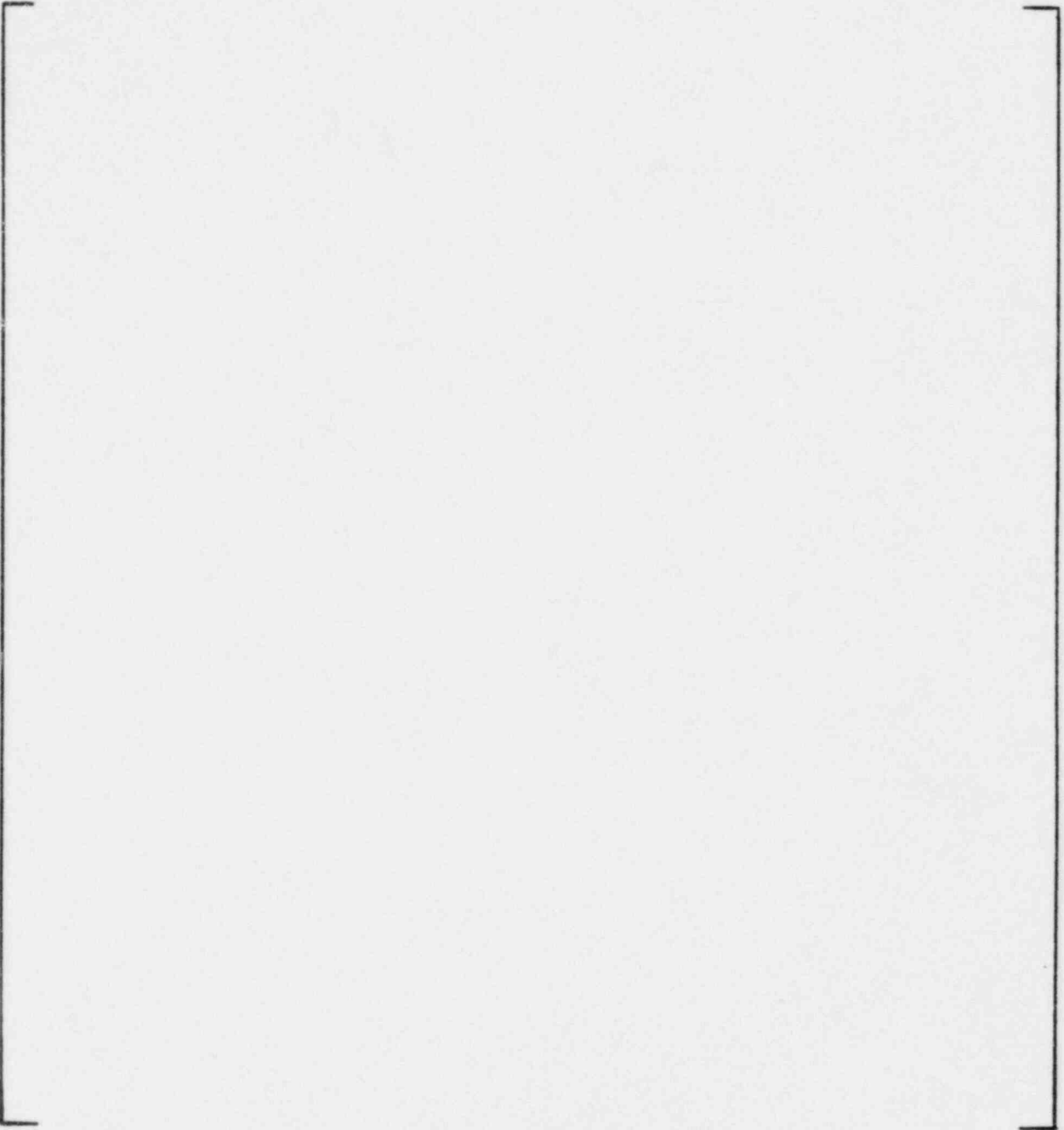


Figure 3-4
HOT ASSEMBLY RADIAL POWER DISTRIBUTION
USED TO GENERATE RESPONSE SURFACE

Figure 3-5

CHANNEL NUMBERING SCHEME FOR STAGE 1 TORC ANALYSIS

NOTE: CIRCLED CHANNEL NUMBER DENOTES
A FLOW CHANNEL IN WHICH SEVERAL
ASSEMBLIES HAVE BEEN "LUMPED" INTO
T-H ANALYSIS

CHANNEL NUMBER
IN FIRST STAGE
TORC

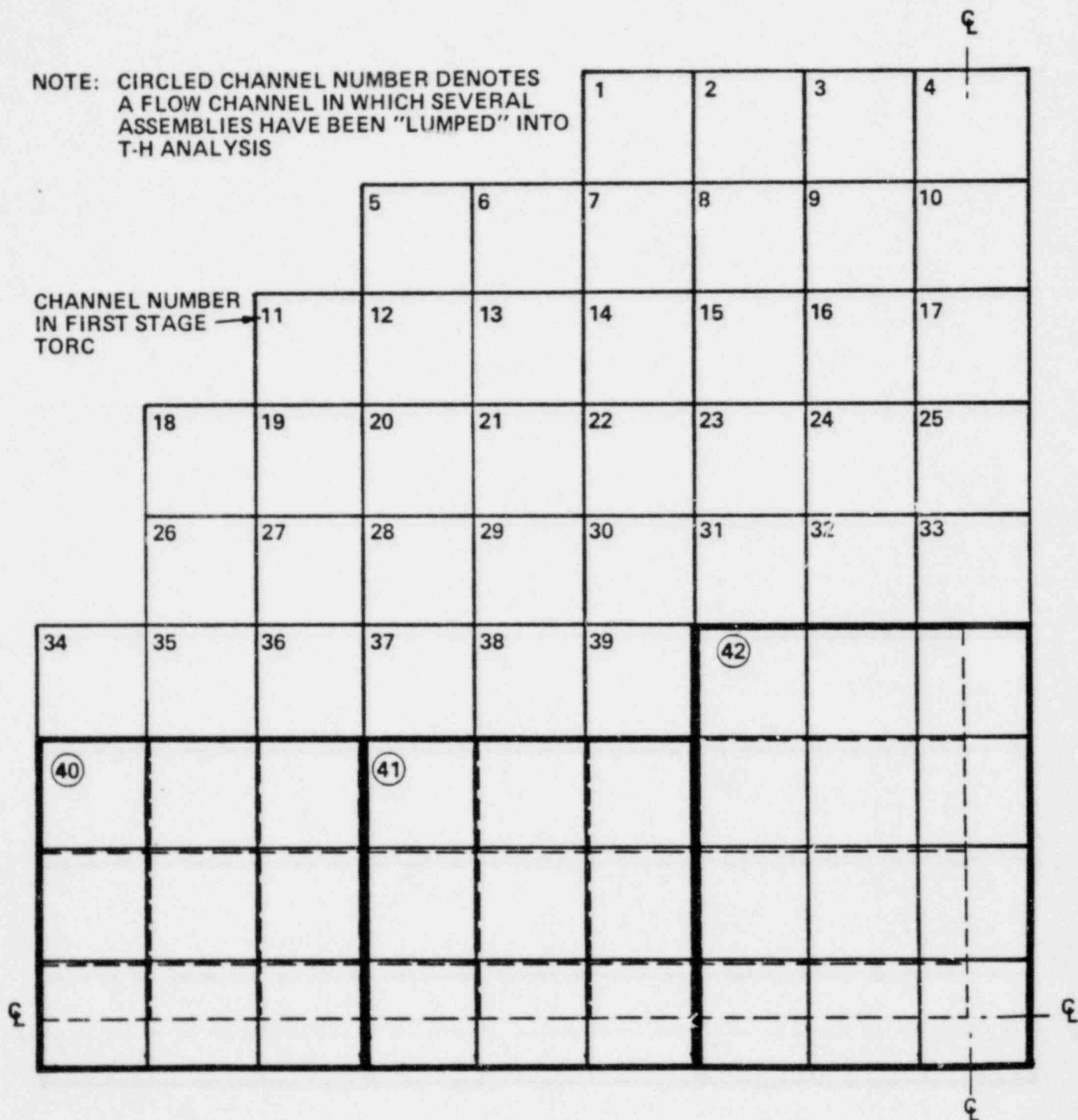


Figure 3-6

INTERMEDIATE (2ND STAGE) TORC MODEL USED IN GENERATING RESPONSE SURFACE

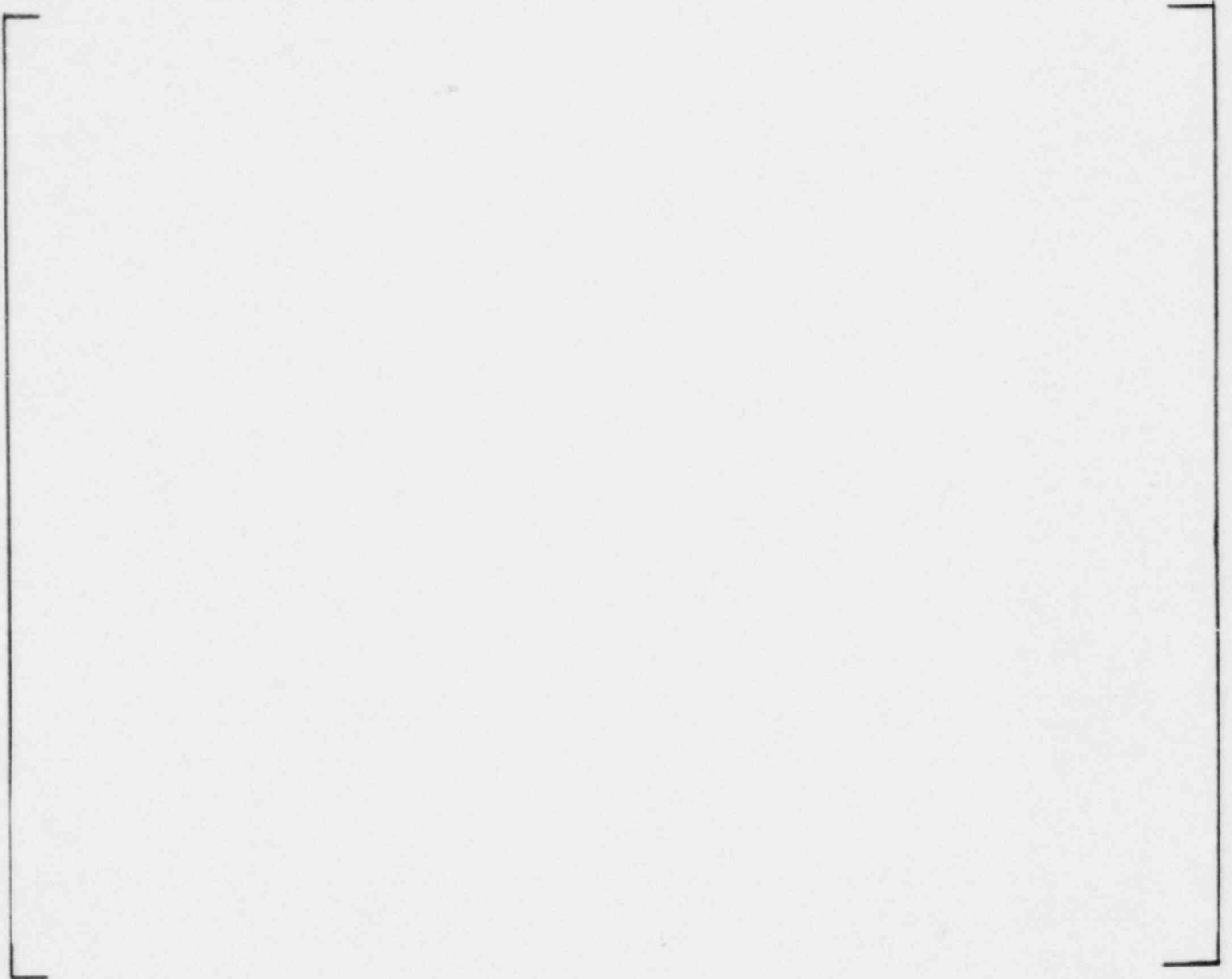


Figure 3-7

SUBCHANNEL (3RD STAGE) TORC MODEL USED IN
GENERATING RESPONSE SURFACE

Operating Conditions	Units	Range
Axial Shape Index	*	$-0.600 \leq \text{A.S.I.} \leq + 0.600$
Inlet Temperature	$^{\circ}\text{F}$	$465 \leq T_{\text{in}} \leq 615$
System Pressure	psia	$1785 \leq P_{\text{sys}} \leq 2400$
System Flow	% Design*	$75 \leq W \leq 120$

NOTES*: See note (1) on Table 3-2 for definition of axial shape index

+ Thermal margin design flow = 445,600 gpm

TABLE 3-1

Ranges of Operating Conditions
for which Response Surface is
Valid

Axial (1) Shape Index	MDNBR			System Parameters Adversely Perturbed	System Parameters Advantageously Perturbed	System Parameters Advantageously Perturbed	+ % Change Adverse % Change Advantageous (2)
	Nominal System Parameters						
+0.636	[
+0.527							
+0.444							
+0.337							
0.000							
-0.001							
-0.055							
-0.064							
-0.070							

TABLE 3-2
Determination of Most Sensitive Axial Shape Index

Axial ⁽¹⁾ Shape Index	MDNBR			Change Adverse + % Change Advantageous ⁽²⁾
	Nominal System Parameters	System Parameters Adversely Perturbed	System Parameters Advantageously Perturbed	
-0.079	[]
-0.094				
-0.317				
-0.359				
-0.527				
-0.636				
-0.094				

$$(1) \text{ Axial Shape Index} = \frac{\int_{-L/2}^0 F_z dz - \int_0^{L/2} F_z dz}{\int_{-L/2}^{L/2} F_z dz}$$

F_z = core average axial peaking factor at axial location z

o = core mid-plane

L = active core length

operating conditions: []

(2) See Section 3

(3) See Section 3.1.1

TABLE 3-2 (cont'd)

Determination of Most Sensitive Axial Shape Index

Press/Temp/Flow (1) psia/°F/% Design	MDNBR			+ % Change Advantageous (2)
	Nominal System Parameters	System Parameters Adversely Perturbed	System Parameters Advantageously Perturbed	
2400/615/75	[]			[]
2400/465/75				
1785/465/75				
2250/565/75				
1785/615/75				
1785/550/75				
2250/565/100				

TABLE 3-3

Determination of Most Sensitive Operating Conditions

Press/Temp/Flow psia/°F/gpm (1)	MDNBR			% Change Adverse + % Change Advantageous (2)
	Nominal System Parameters	System Parameters Adversely Perturbed	System Parameters Advantageously Perturbed	
1785/550/100	[]	[]	[]	[]
2400/615/120				
2400/465/120				
2250/565/120				
1785/615/120				
1735/550/120				
1785/465/120				
(1) Design Flow = 445,600 gpm				Axial Shape Index Used: []
(2) See Section 3.1.1				

TABLE 3-3 (cont'd)

Determination of Most Sensitive Operating Conditions

Span Number	Assembly Identification				
	AKA050	AKA051	AKBT01	AKBT02	AKC107
10					
6					
2					

Mean + xxxx(xxx) + number of measurements

xxxx + standard deviation of mean

TABLE 3-4

As-Built Gap Width Data (inches)

INLET MASS VELOCITY RATIO

Fuel Assembly Number*		
[]

TABLE 3-5

*Assembly numbers refer to Figure 3-5

4.0 MDNBR Response Surface

A response surface is a functional relationship which involves several independent variables and one dependent variable. The surface is created by fitting the constants of an assumed functional relationship to data obtained from "experiments".

The response surface provides a convenient means by which accurate estimates of a complex or unknown function's response may be obtained. Since the response surface is a relatively simple expression, it may be applied in analytic techniques where more complex functions would make an analytic solution intractable.

In the present application, a single detailed TORC analysis is treated as an "experiment". A carefully selected set of detailed TORC "experiments" is conducted, and a functional relationship is fitted to the MDNBR results. This response surface is then used in conjunction with Monte Carlo techniques to combine probability distribution functions (p.d.f.'s) for each of the independent variables into a resultant MDNBR p.d.f.

4.1 TORC Model Used

The inlet flow distribution (shown in Fig. 3-1) is compared with radial power distributions to determine the limiting location for DNB analysis. For the purpose of generating the response surface, the limiting location is defined as the assembly in which the impact of system parameter uncertainties on MDNBR is the greatest. The core-wide and limiting assembly radial power distributions used to generate the response surface are shown in Figs. 3-3 and 3-4, respectively.

The first stage TORC model used in this analysis is shown in Fig. 3-5. The limiting assembly occurs in channel of this model. Second and third stage models used in this analysis are shown in Figs. 3-6 and 3-7, respectively.

4.2 Variables Used

A careful examination of the sources of uncertainty discussed in Section 3 shows that several of these sources of uncertainty can be omitted from the response surface.

As explained in Section 3.2, inherent conservatism in the thermal margin modelling methodology factors makes it unnecessary to account for uncertainty in the radial power distribution used in DNB analyses. Hence, the radial power distribution was omitted from the response surface.

Since the inlet flow distribution uncertainties are taken into account using deterministic methods, as explained in Section 3.3, these uncertainties are not included in the statistical analysis.

The sensitivity study discussed in Section 3.4 indicates that large perturbations in the exit pressure distribution have negligible effect on the predicted MDNBR. Thus, the exit pressure distribution is not included in the response surface.

The heat flux factor ($F_{q''}$) is applied to the MDNBR calculated by TORC in the following manner:

$$\text{MDNBR} = \frac{\text{MDNBR}_{\text{TORC}}}{F_{q''}} \quad (4.1)$$

Since the functional relationship between MDNBR and $F_{q''}$ is known, the heat flux factor is not used in generating the response surface. Instead, this factor is combined with the resultant surface, as explained in Section 4.5.

A method has already been developed (4-1) to account for rod bow uncertainty. No rod bow effects are included in the response surface. Instead, the rod bow penalty determined with existing methods (4-1) is applied to the design limit MDNBR as discussed in Section 6.2.

The calculational uncertainty associated with MDNBR predictions using the TORC/CE-1 package is implicitly included in the CHF distribution uncertainty, as explained in Sections 3.10 and 3.11. Hence no explicit allowance for code uncertainty is included in the response surface.

The system parameters included as variables in the response surface are listed in Table 4-1.

4.3 Experimental Design

An orthogonal central composite experimental design (4-2) is used to generate the response surface applied in this study. The total number of experiments needed to generate a response surface using this experiment design is

$$2^k + 2k + 1$$

where k is the number of variables to be considered. The desired response surface consists of three variables, hence 15 "experiments" or detailed TORC analyses were needed for a full orthogonal central composite design. The results of these experiments may then be manipulated by means of the least squares estimator

$$\underline{b} = (\underline{n}' \underline{n})^{-1} \{\underline{n}'\} \underline{z} \quad (4.2)$$

where \underline{z} is the vector of experimental results, to yield the coefficients which define the response surface.

$$\underline{z} = \text{MDNBR}_{\text{RS}} = b_0 + \sum_{i=1}^3 b_i n_i + \sum_{i=1}^3 b_{ii} (n_i^2 - c) + \sum_{i=1}^3 \sum_{\substack{j=1 \\ i < j}}^3 b_{ij} n_i n_j \quad (4.3)$$

In the above equations, the n_i are coded values of the system parameters (x_i) to be treated in the response surface, as indicated in Table 4-1.

The b_i represent the constants found from the TORC results by means of Eq. 4.2, and c is a constant determined from the number of experiments conducted.

The number of TORC analyses needed to generate the response surface could be reduced significantly if some of the interaction effects (i.e., $b_{ij}n_i n_j$) were neglected. However, such interaction effects are included in the present method.

4.4 Design Matrix

The set of experiments used to generate the response surface is referred to as the design matrix. This matrix, in coded form, comprises the second through fourth columns of the matrix cited in Eq. (4.2). Both coded and uncoded versions of the design matrix used in this study are presented in Appendix A along with resultant MDNBR values. The design matrix was constructed such that each independent variable included in the response surface extends just beyond the 2σ range of its associated p.d.f.

4.5 Response Surface

Equation (4.2) was solved numerically using the data in Appendix A.

Coefficients for the response surface as given by Eq. (4.3) are presented in Table 4-2. Comparisons made between TORC predicted MDNBR and response surface predictions show excellent agreement. The 95% confidence estimate of the response surface standard deviation is 0.00357.

The heat flux factor is included analytically in the response surface by combining Eq. (4.1) with Eq. (4.3). The final relationship is given by

$$\text{MDNBR} = \frac{1}{F_q''} \left\{ b_0 + \sum_{i=1}^3 b_i n_i + \sum_{i=1}^3 b_{ii} (n_i^2 - c) + \sum_{\substack{i=1 \\ i < j}}^3 \sum_{j=1}^3 b_{ij} n_i n_j \right\} \quad (4.4)$$

The coefficient of determination, r , provides an indication of how well the response surface explains the total variation in the response variable (4-3). When $r = 1$, a true model has been found. The r value associated with the response surface generated in this work is 0.99912 which indicates that this response surface is a good model.

Another indication of model performance is provided by the standard error of estimate (4-4). The standard error for the response surface is 0.001711. The relative error is 0.17% indicating that this model performs well.

System Parameter	Variable	Index (i)	Coded Values*	
			α_i	β_i
Enthalpy Rise Factor	X_1	1	[]
Systematic Pitch (Inches)	X_2	2		
Systematic Clad O.D. (Inches)	X_3	3		

*variables coded according to relation $n_i = \frac{X_i - \alpha_i}{\beta_i}$ where the α_i are chosen such that $n_i = 0$ at nominal conditions and the β_i are chosen such that the interval of the response surface will include $\sim 2\sigma$ intervals of each of the system parameters.

TABLE 4-1
System Parameters Included as Variables in
the Response Surface

Response Surface Coefficients	Coefficient Values
b_0	[
b_1	
b_2	
b_3	
b_{11}	
b_{22}	
b_{33}	
b_{12}	
b_{13}	
b_{23}	
c	

$$MDNBR_{R.S.} = b_0 + \sum_{i=1}^3 b_i n_i + \sum_{i=1}^3 b_{ii} (n_i^2 - c) + \sum_{i=1}^3 \sum_{j=1}^3 b_{ij} n_i n_j$$

TABLE 4-2

Coefficients for MDNBR Response Surface

5.0 Combination of Probability Distribution Functions

The MDNBR response surface discussed in Section 4 is applied in Monte Carlo methods to combine numerically the system parameter probability distribution functions (p.d.f.'s) discussed in Section 3 with the CHF correlation uncertainty. A new 95/95 MDNBR limit is then selected from the resultant p.d.f. This new limit includes the effect of system parameter uncertainties and thus may be used in conjunction with a best estimate design TORC model.

5.1 Method

The SIGMA code applies Monte Carlo and stratified sampling techniques to combine arbitrary p.d.f.'s numerically (5-1). This code is used with the response surface to combine system parameter p.d.f.'s with the CE-1 CHF correlation p.d.f. into a resultant MDNBR p.d.f. The methods used to achieve this combination are discussed below.

The effect of system parameter uncertainties on MDNBR is combined with the effect of uncertainty in the CHF correlation by computing a Δ MDNBR caused by deviation of the system parameters from nominal:

$$\Delta \text{MDNBR} = \text{MDNBR}_{R.S.} - \text{MDNBR}_{\text{NOM}} \quad (5.1)$$

where $\text{MDNBR}_{R.S.}$ is the MDNBR found by substituting the set of system parameters into the response surface and $\text{MDNBR}_{\text{NOM}}$ is the MDNBR value predicted by the response surface with nominal system parameters. A point is then randomly chosen from the CHF correlation p.d.f. and combined with the MDNBR from Eq. (5.1) to yield a MDNBR value:

$$\text{MDNBR} = \text{MDNBR}_{\text{CHF}} + \Delta \text{MDNBR} \quad (5.2)$$

This process is repeated by the SIGMA code for 2000 randomly selected sets of system parameters and randomly selected points from the CHF correlation p.d.f., and a resultant MDNBR p.d.f. is generated.

The system parameter p.d.f.'s input to SIGMA are listed in Table 5-1. Both "best estimate" and 95% confidence estimates of the standard deviation are included. Standard deviations at the 95% confidence level are input to SIGMA to ensure that the standard deviation of the resultant MDNBR p.d.f. is at least at the 95% confidence limit.

5.2 Results

The resultant MDNBR p.d.f. is shown in Fig. 5-1. The mean and standard deviation of this p.d.f. are 1.00568 and 0.0739714 respectively. As Fig. 5-1 indicates, the resultant MDNBR p.d.f. approximates a normal distribution.

5.3 Analytical Combination

An approximate value of the standard deviation of the resultant MDNBR p.d.f. may be found by analytic methods. These methods are based upon the

assumption that the uncertainties are small deviations from the mean (5-2). Given a functional relationship

$$y = f(x_1, x_2, \dots, x_n) \quad (5.3)$$

the effects of small perturbations in x on y may be found from

$$\Delta y \simeq dy \simeq \left(\frac{\partial f}{\partial x_1}\right) \Delta x_1 + \left(\frac{\partial f}{\partial x_2}\right) \Delta x_2 + \dots + \left(\frac{\partial f}{\partial x_n}\right) \Delta x_n \quad (5.4)$$

Hence, if several independent normal distributions are combined by the relationship expressed in Eq. (5.3), the variance of the resultant p.d.f. is

$$\sigma_y^2 \simeq \left(\frac{\partial f}{\partial x_1}\right)^2 \sigma_{x_1}^2 + \left(\frac{\partial f}{\partial x_2}\right)^2 \sigma_{x_2}^2 + \dots + \left(\frac{\partial f}{\partial x_n}\right)^2 \sigma_{x_n}^2 \quad (5.5)$$

where the partial derivatives are evaluated at the mean value of the x_i 's.

The response surface relates MDNBR to system parameters by the relationship found on Table 4-2:

$$\text{MDNBR}_{\text{RS}} = b_0 + \sum_{i=1}^3 b_i \eta_i + \sum_{i=1}^3 b_{ii} (\eta_i^2 - c) + \sum_{i=1}^3 \sum_{\substack{j=1 \\ i < j}}^3 b_{ij} \eta_i \eta_j \quad (5.6)$$

$$\text{where } \eta_i = \frac{x_i - \alpha_i}{\beta_i} \quad (5.7)$$

Applying Eq. 5.5 to the response surface yields the following expression for the variance:

$$\sigma_{\text{RS}}^2 = \sum_{i=1}^3 \left(\frac{\partial(\text{MDNBR})}{\partial \eta_i} \frac{\partial \eta_i}{\partial x_i} \right)^2 \sigma_{x_i}^2 \quad (5.8)$$

Differentiating Eq. (5.6) and (5.7) with respect to η_i and x_i :

$$\frac{\partial \text{MDNBR}}{\partial \eta_i} = b_i + 2b_{ii} \eta_i + \sum_{j=i+1}^3 b_{ij} \eta_j \quad (5.9)$$

$$\frac{\partial \eta_i}{\partial x_i} = \frac{1}{\beta_i} \quad (5.10)$$

Substituting Eq. (5.9) and (5.10) into Eq. (5.8) results in a relation between the resultant MDNBR variance and the system parameter variances:

$$\sigma_{\text{RS}}^2 = \sum_{i=1}^3 \left(b_i + 2b_{ii} \eta_i + \sum_{j=i+1}^3 b_{ij} \eta_j \right)^2 \left(\frac{\sigma_{x_i}}{\beta_i} \right)^2 \quad (5.11)$$

This equation is simplified when evaluated at the mean values of the n_i : (i.e., $n = 0$)

$$\sigma_{RS}^2 = \sum_{i=1}^3 b_i^2 \frac{\sigma_{x_i}^2}{\beta_i^2} \quad (5.12)$$

The CHF correlation p.d.f and system parameter p.d.f.'s are related to the resultant MDNBR in Eq. (5.1) and Eq. (5.2), and the heat flux factor is related by Eq. (4.1). The resultant MDNBR variance is given by

$$\frac{\sigma_{MDNBR}^2}{\mu_{MDNBR}^2} = \frac{\sigma_{R.S.}^2 + \sigma_{CHF}^2}{(\mu_{R.S.} + \mu_{CHF})^2} + \frac{\sigma_{Fq''}^2}{\mu_{Fq''}^2} \quad (5.13)$$

where

$$\mu_{R.S.}^2 \approx 0$$

Substituting values from Tables 4-1, 4-2, 5-1, and Section 4.5 into Eq. (5.11) and Eq. (5.13) yields:

$$\sigma_{MDNBR} = .07694$$

which is in excellent agreement with the value predicted by the SIGMA code simulation using the response surface.

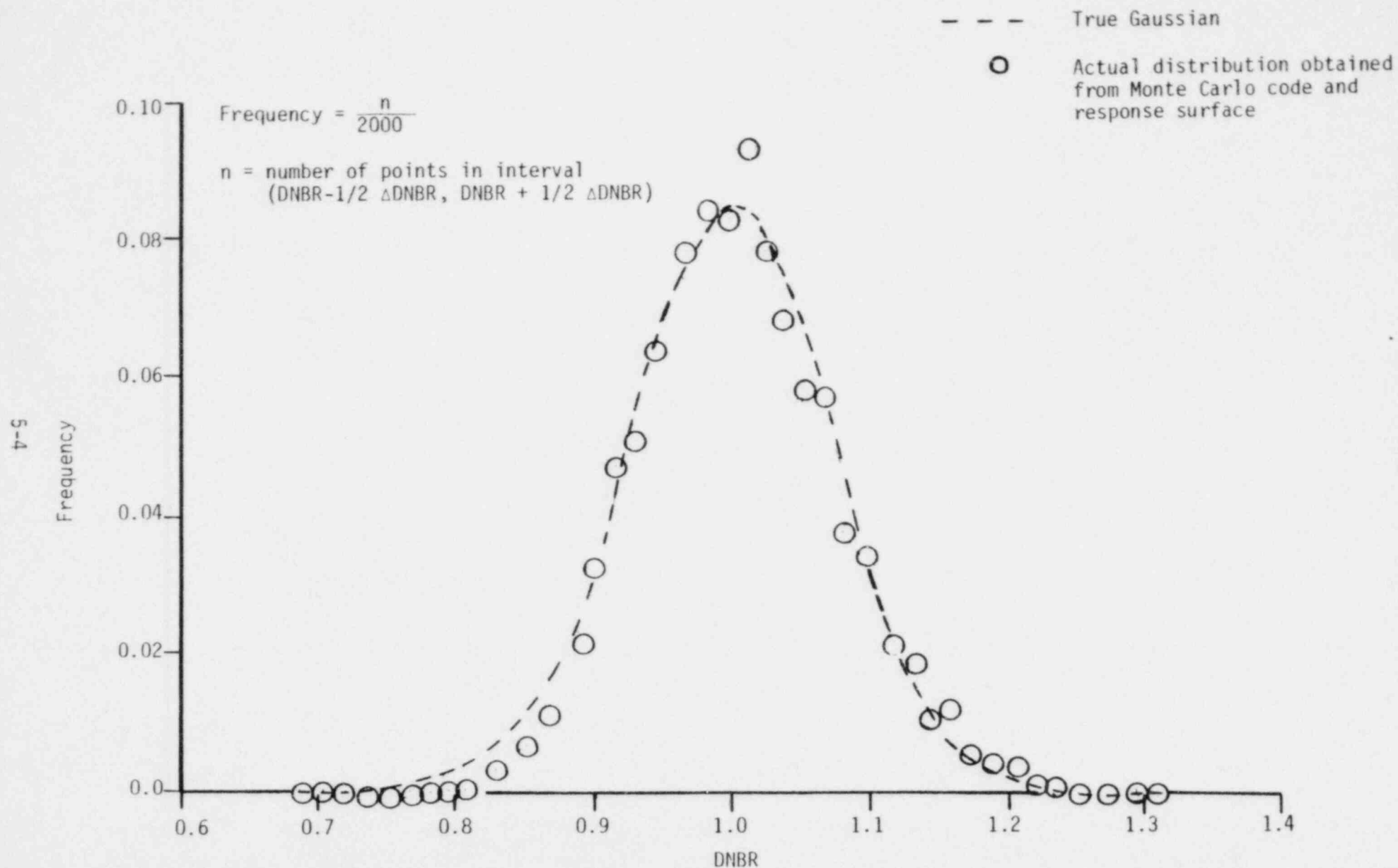


Figure 5-1

Resultant MDNBR Probability Distribution Function

Distribution	Mean	Standard Deviation at 95% Confidence
Enthalpy Rise Factor Systematic h (in) Systematic ad OD (in) Heat Flux Factor CE-1 CHF Correlation	[]

TABLE 5-1

Probability Distribution Functions
Combined by SIGMA

6.0 Application to Design Analysis

This section discusses the application of the statistically derived MDNBR p.d.f to design analyses. Deterministic methodology (6-1) involves use of a design model for TORC analysis which includes deterministic allowances for system parameter uncertainties. These deterministic penalties are replaced with a higher MDNBR limit in the statistical methodology. This higher MDNBR limit is used with a "best estimate" design model in thermal margin analyses.

6.1 Statistically Derived MDNBR Limit

The MDNBR p.d.f described in Section 5.0 is a normal distribution having a mean of 1.00568 and a standard deviation of 0.073971. This standard deviation is at least at the 95% confidence level. A comparison of TORC results and response surface predictions indicates that the 1 error associated with the response surface is $\sigma_s = 0.0011711$; at the 95% confidence level, this value is $\sigma_{s95} = 0.001939 \times \sqrt{5/1.15} = .00404$.

The MDNBR standard deviation was found to be 0.073971 by means of Monte Carlo methods. Since a finite number of points (2000) were used in these methods, a correction must be applied to the calculated value. The resultant MDNBR standard deviation, adjusted for the finite sample size used is $0.073971 \times 1999/1896.131 = 0.075952$. The root sum square of the adjusted MDNBR standard deviation and the response surface standard deviation at the 95% confidence level is:

$$\sigma_{\text{tot}} = \sqrt{(0.075952)^2 + (0.00404)^2} = 0.076059. \text{ The}$$

corresponding 95% confidence estimate of the mean is

$$(1.00568 + (1.645 \times .073971) / \sqrt{2000}) = 1.00840$$

Since the resultant MDNBR p.d.f. is a normal distribution, as shown in Figure 5-1, the one-sided 95% probability limit is 1.645σ . Hence there is a 95% probability with at least 95% confidence that the limiting fuel pin will not experience DNB if the best estimate design model TORC calculation yields a MDNBR value greater than or equal to $(1.00840 + 1.645 (.076059)) = 1.1335$

6.2 Adjustments to Statistically Derived MDNBR Limit

The statistical MDNBR limit derived in Section 6.1 contains no allowance for the adverse impact on DNBR of fuel rod bowing. C-E has applied an NRC method for taking rod bow into account in DNBR calculations (6-2). This application shows that the penalty depends on batch average burnup. For 16x16 fuel, this penalty is 0.80% in MDNBR at a burnup of 20 GWD/MTU. Batch average burnups for Cycle 1 will not exceed 20 GWD/MTU. Thus, the new limit, including an allowance for rod bow is (1.008×1.1335) or 1.1425.

This new MDNBR limit does not include the .01 NRC imposed DNBR penalty for the use of HID grids. With this penalty the new limit, including allowance for the HID grid loss is 1.1525.

The NRC has not yet completed review of the application of the CE-1 CHF

correlation (6-3) to non-uniform axial heat flux shape data (6-4). Consequently, a 5% penalty was applied to the 1.13 MDNBR limit by the NRC. The interim MDNBR limit for use with the CE-1 CHF correlation, pending NRC approval of C-E's non-uniform axial heat flux shape data, is 1.19. For the purposes of this study, a conservative application of this penalty is to shift the mean of the MDNBR p.d.f. by 0.06. This shift results in a MDNBR limit of 1.213, rounded up to 1.22.

Thus, the new MDNBR limit which contains allowances for uncertainty in the CHF correlation and system parameters as well as a 0.8% rod bow penalty, the NRC imposed DNBR MID grid loss penalty, and the NRC imposed 5% CE-1 correlation penalty is 1.22.

6.3 Application to TORC Design Model

Statistical combination of system parameter uncertainties into the MDNBR limit precludes the need for deterministic application of penalty factors to the design TORC model. The design TORC model used with the new MDNBR limit of 1.22 consists of best estimate system parameters with no engineering factors or other adjustments to accommodate system parameter uncertainties. The inlet flow split will, however, continue to be chosen such that the best estimate design TORC model will yield accurate or conservative MDNBR predictions when compared with MDNBR values from detailed TORC analyses (6-1) which include deterministic allowances for inlet flow distribution uncertainties.

7.0 Conclusions

Use of a 1.22 MDNBR limit with a best-estimate design CETOP-D model for System 80 will ensure with at least 95% probability and 95% confidence, that the hot pin will not experience a departure from nucleate boiling. The 1.22 MDNBR limit includes explicit allowances for system parameter uncertainties, CHF correlation uncertainty, rod bow, the NRC penalty, for the HID spacer grids and the 5% interim penalty imposed by the NRC on the CE-1 CHF correlation.

7.1 Conservatisms in the Methodology

Several conservatisms are included in the present application. The significant conservatisms include:

- i) combination of system parameter p.d.f.'s at the 95% confidence level to yield a resultant MDNBR at a 95% + confidence level
- ii) use of pessimistic system parameter p.d.f.'s
- iii) use of the single most adverse set of state parameters to generate the response surface
- iv) application of the 5% interim penalty imposed by the NRC on the CE-1 CHF correlation
- v) application of the 0.01 HID grid penalty imposed by the NRC on the CE-1 CHF correlation.

8.0 References

8.1 Section 2.0 References

- (2-1) "TORC Code: Verification and Simplified Modeling Models", CENPD-206-P, January 1977.
- (2-2) "TORC Code: A Computer Code for Determining the Thermal Margin of a Reactor Core", CENPD-161-P, July 1975.
- (2-3) "CETOP-D Code Structure and Modeling Methods for San Onofre Nuclear Generating Station Units 2 and 3", CEN-160(S)-P, Rev. 1-P, Docket No. 50-361, 50-362, Sept. 1981.
- (2-4) "C-E Critical Heat Flux: Critical Heat Flux Correlation for C-E Fuel Assemblies with Standard Grids, Part 1: Uniform Axial Power Distribution", CENPD-162-P, September 1976.

8.2 Section 3.0 References

- (3-1) "TORC Code: A Computer Code for Determining the Thermal Margin of a Reactor Core, CENPD-161-P, July 1975, pp. 5-1 to 5-8.
- (3-2) "Combustion Engineering Standard Safety Analysis Report, (System 80), Docket #STN-50-470F, October 26, 1979, Fig. 4.4-7.
- (3-3) ibid, Subsection 4.4.2.2.2.2.C.
- (3-4) "Statistical Combination of Uncertainties, Part 2", CEN-124(B)-P, January 1980.
- (3-5) Green & Bourne, "Reliability Technology", Wiley-Interscience, A Division of John Wiley & Sons Ltd., p. 326.
- (3-6) "Fuel and Poison Rod Bowing", CENPD-225-P, October 1976.
- (3-7) "Fuel and Poison Rod Bowing - Supplement 3", CENPD-225-P, Supplement 3, June 1979.
- (3-8) Letter from D. B. Vassallo (NRC) to A. E. Scherer (C-E), June 12, 1978.
- (3-9) "CE Critical Heat Flux: Critical Heat Flux Correlation for CE Fuel Assemblies with Standard Spacer Grids, Part 1: Uniform Axial Power Distribution", CENPD-162-P, September 1976.
- (3-10) "C-E Critical Heat Flux: Critical Heat Flux Correlation for C-E Fuel Assemblies with Standard Spacer Grids, Part 2: Nonuniform Axial Power Distribution", CENPD-207-P, June 1976.
- (3-11) "TORC Code: Verification and Simplified Modeling Methods", CENPD-206-P, January 1977.

8.3 References for Section 4

- (4-1) "Fuel and Poison Rod Bowing, Supplement 3", CENPD-225-P, June 1979.
- (4-2) R. H. Myers, Response Surface Methodology, Allyn and Bacon, Inc. Boston, 1971.
- (4-3) N. R. Draper, H. Smith, Applied Regression Analysis, John Wiley & Sons, New York, 1966, p. 62.
- (4-4) *ibid.*, p. 118

8.4 References for Section 5

- (5-1) F. J. Berte, "The Application of Monte Carlo and Bayesian Probability Techniques to Flow Prediction and Determination", Combustion Engineering Technical Paper TIS-5122, presented at the Flow Measurement Symposium, sponsored by the National Bureau of Standards, Gaithersburg, Maryland, February 23-25, 1977.
- (5-2) E. L. Crow, F. A. Davis, M. W. Maxfield, Statistical Manual, Dover Publications, Inc., New York, 1960.

8.5 References for Section 6

- (6-1) "TORC Code: Verification and Simplified Modeling Methods", CENPD-206-P, January 1977.
- (6-2) "Fuel and Poison Rod Bowing, Supplement 3", CENPD-225-P, Supplement 3-P, June 1979.
- (6-3) "C-E Critical Heat Flux: Critical Heat Flux Correlation for C-E Fuel Assemblies with Standard Spacer Grids, Part 1: Uniform Axial Power Distribution", CENPD-162-P, September 1976.
- (6-4) "C-E Critical Heat Flux; Critical Heat Flux Correlation for C-E Fuel Assemblies with Standard Spacer Grids, Part 2: Nonuniform Axial Power Distribution", CENPD-207-P, June 1976.

Appendix A: Detailed TORC Analyses Used To Generate Response Surface

An orthogonal central composite experimental design (A-1) was used to generate the response surface (R S) used in this study. All first order interaction effects (i.e. $x_i x_j$ terms) were retained in the R S. The R S used in this study included three variables. The coded set of detailed TORC analyses performed to generate the R S is presented in Table A-1; variables were coded as shown in Table 4-1. The actual values of the input parameters are presented in Table A-2 along with the resultant MDNBR values.

References

- (A-1) R. H. Myers, Response Surface Methodology, Allyn & Bacon, Inc., Boston, 1971, p. 133.

Case Number	Enthalpy Rise Factor	Systematic Pitch	Systematic Clad O.D.
1	-1.00	-1.00	-1.00
2	-1.00	-1.00	-1.00
3	-1.00	1.00	-1.00
4	-1.00	1.00	1.00
5	1.00	-1.00	-1.00
6	1.00	-1.00	1.00
7	1.00	1.00	-1.00
8	1.00	1.00	1.00
9	0.00	0.00	0.00
10	-1.22	0.00	0.00
11	1.22	0.00	0.00
12	0.00	-1.22	0.00
13	0.00	1.22	0.00
14	0.00	0.00	-1.22
15	0.00	0.00	1.22

See Table 4-1 for Coded Relationships

TABLE A-1

Coded Set of Detailed TORC Cases
Used to Generate Response Surface

Case Number	Enthalpy Rise Factor	Systematic Pitch	Systematic Clad O.D.	Detailed TORC MDNBR	Response TORC MDNBR	Residual
1						
2						
3						
4						
5						
6						
7						
8						
9						
10						
11						
12						
13						
14						
15						

TABLE A-2
Comparison of TORC and Response Surface MDNBR for Cases
Used to Generate Response Surface